



OPEN

# Mechanical and viscoelastic properties of a temperature-responsive photocurable resin for 3D printed orthodontic clear aligners

Jin Young Choi<sup>1,6</sup>, Hoon Kim<sup>2,5,6</sup>, Seong Hun Kim<sup>1</sup>, Su Jung Kim<sup>1</sup>, Jung-Yul Cha<sup>3</sup>, Se Yeon Lee<sup>3</sup>, Jiho Lee<sup>5</sup>, Jinhong Min<sup>5</sup>, Sunho Jang<sup>5</sup>, Tanveer Ahmed Khan<sup>5</sup>, Hyun-Joong Kim<sup>2</sup> & Ki Beom Kim<sup>4</sup>✉

This study investigates the mechanical and viscoelastic properties of TC-85, a biocompatible material specifically designed for orthodontic applications, with a focus on how temperature variations influence its mechanical and viscoelastic properties and their relevance to clinical outcomes. Using a Digital Light Processing (DLP) 3D printer, the photosensitive resin TC-85 is printed, and extensive thermo-mechanical testing is conducted, which includes evaluations of tensile modulus, stress relaxation, and creep behavior. Dynamic Mechanical Analysis (DMA) is conducted at temperatures varying from 30 to 45 °C to assess the material's adaptive response to thermal fluctuations. TC-85 is distinguished by its unique mechanical properties, which include a temperature-sensitive stiffness, stress relaxation capability, and shape memory feature. The results demonstrate that TC-85 maintains an enhanced level of residual force and a faster recovery of strain through numerous cycles of loading and unloading. At 40 °C, TC-85 displays a substantial reduction in its storage modulus, while maintaining consistent strain recovery and volumetric constancy. The study highlights TC-85's potential in orthodontic treatments, providing adaptable mechanical and viscoelastic properties that enable the exertion of consistent and regulated forces on teeth. Its resistance to force decay, stable volume at raised temperatures, and shape memory properties enhance hygienic maintenance and patient comfort, positioning TC-85 as a pioneering material for the next generation of clear aligners.

Clear aligners have become increasingly prevalent in orthodontics. The global clear aligners market size was valued at USD 3.80 billion in 2023 and is projected to grow from USD 4.66 billion in 2024 to USD 28.15 billion by 2032, exhibiting a CAGR of 25.2% during the forecast period 2024–2032. North America dominated the clear aligners market with a market share of 56.05% in 2023<sup>1,2</sup>. Their appeal to patients lies in their aesthetic discretion and comfort, while orthodontists benefit from reduced chair time and simplified oral hygiene management<sup>3</sup>. Even with increased applications of clear aligners, clear aligners are considered less effective for achieving certain tooth movements, such as buccolingual tilting, extraction space closure and palatal expansion, compared to conventional fixed appliances<sup>4,5</sup>. Additionally, clear aligners are often found to be less successful in correcting major anteroposterior discrepancies<sup>6</sup>.

Since the invention of clear aligner orthodontic treatment until now, the most commonly used material for conventional thermoforming clear aligners is polyethylene terephthalate glycol (PETG), followed by thermoplastic polyurethanes (TPU), polycarbonate (PC), polypropylene (PP), copolyester, and others<sup>7–11</sup>. Although PETG is very effective in exerting a strong force on teeth, it does not provide the moderate and sustained force preferred for orthodontic treatments<sup>12</sup>. Additionally, the fitting accuracy of aligners produced from these materials are

<sup>1</sup>Department of Orthodontics, Graduate School, Kyung Hee University, Seoul 02447, Republic of Korea. <sup>2</sup>College of Agriculture and Life Sciences, Research Institute of Agriculture and Life Sciences, Seoul National University, Seoul, Republic of Korea. <sup>3</sup>Department of Orthodontics, Institute of Craniofacial Deformity, College of Dentistry, Yonsei University, Seoul, Republic of Korea. <sup>4</sup>Department of Orthodontics, Saint Louis University, St. Louis, USA. <sup>5</sup>Graphy, Inc., Seoul, Republic of Korea. <sup>6</sup>These authors contributed equally: Jin Young Choi and Hoon Kim. ✉email: kibeam.kim@health.slu.edu

often not ideal due to the constraints of the heat fusion process<sup>13,14</sup>. Despite attempts to enhance precision through multi-layered urethane/PETG structures, the intrinsic properties of the thermoplastic materials after heat treatment process pose challenges in achieving the optimal accuracy<sup>13,15–23</sup>. The direct 3D printing of clear aligners with urethane-acrylic photocurable resins represents a breakthrough, offering improvements in the rheological properties (viscosity and elasticity suitable for orthodontic treatment) and superior fit accuracy compared to the conventional vacuum formed clear aligners<sup>14,22,24–31</sup>. As a spotlighted technology for dental products, 3D printing, especially VAT photopolymerization based 3D printing, such as SLA (Stereolithography), DLP (digital light processing), and LCD, making its way into direct printing of clear aligners is not surprising after all, as the technology has promised and proven itself with its high-quality resolution as well as functional and smart material applications<sup>30,32–35</sup>. For polymers as such, in-depth analysis on their rheological properties is required for thorough understanding of the material.

Various static mechanical properties of existing thermoplastics, including water absorption, solubility, surface hardness, transparency, fatigue, creep, and stress relaxation, have been extensively evaluated in numerous studies<sup>7,36–39</sup>. These investigations have subsequently paved the way for numerous clinical case studies aimed at optimizing the application of clear aligners in clinical practice<sup>26,40–44</sup>. Among a multitude of physical attributes, enhancing device performance and predicting treatment outcomes necessitate a comprehensive understanding of not only static mechanical properties but also force decay due to creep and stress relaxation<sup>12,39,45,46</sup>. This importance stems from the prolonged wear and the repetitive attachment and detachment of clear aligners during orthodontic treatment<sup>37,39,46</sup>. In contrast to elastic materials like Ni-Ti wire, the plastics used in clear aligners exhibit viscoelastic properties, existing in an intermediate state between viscous and elastic materials<sup>47</sup>. This viscoelastic nature allows clear aligners to withstand prolonged loading, displaying distinct behaviors depending on the applied load<sup>48</sup>. Creep behavior is characterized by gradual deformation under a repeated and constant load, leading to a decrease in restoring force as the deformation continues. Previous research has indicated that stress relaxation, ranging from 17.9% to 62%, occurs over a 24-h period under conditions simulating the oral cavity (37 °C and 100% humidity)<sup>49</sup>. The degree of relaxation varies with the type of thermoplastic material and the number of layers used, according to empirical evidence<sup>49</sup>.

Although the mechanical characteristics of directly printed clear aligners may seem inferior to those manufactured by using thermoforming due to its smaller force as found in some studies thickness variation and shape memory property can be advantages in more detailed control over orthodontic force<sup>12,50</sup>. When a gentler correction force is needed for tooth alignment, the mechanical properties of the material can be customized by adjusting the temperature or by altering the thickness of the direct printed aligners at the 3D design stage. The 3D direct printed aligners are thermo-responsive, thus react to temperature change immediately which could be used to ease pain or discomfort the patient may experience during the treatment.

In the prior study, the thermo-mechanical and viscoelastic properties were analyzed at 37 °C and 80 °C<sup>39</sup>. However, the oral temperature in clinical situation is seldom sustained at 37 °C (body temperature) and rarely reaches the exceptionally high level of 80 °C. Instead, the temperature within the oral cavity varies within a smaller range with consumption of food, drinks, and other factors. In fact, according to a study conducted on temperature variations in oral cavity, the resting mouth temperature varied between 29.9 and 36.8 °C<sup>51</sup>. Therefore, it is important to analyze the properties of the aligners in response to the range of temperatures that aligns more with the actual oral temperatures that the users encounter throughout the day.

This study aimed to investigate the changes in mechanical properties relative to temperature. Tensile strength, rheological properties, and creep recovery were measured at more precise temperatures (25 °C, 30 °C, 35 °C, and 40 °C) by immersing specimens in a temperature-controlled water bath. An analysis of the clinical implications was then carried out based on these comprehensive results.

## Material & method

### Specimen preparation

The material chosen for the direct-printed aligners was TC-85, obtained from Graphy Inc. in Seoul, Korea. Formulated from the oligomers GR30860 and GR3060, this resin undergoes polymerization with the addition of bis(2,4,6-trimethylbenzoyl)-phenylphosphine oxide as a photoinitiator, known commercially as Irgacure 819 (BASF SE, Ludwigshafen, Germany). Approved by FDA 510(k) and CE class IIa, the material's major component is an aliphatic urethane acrylate oligomer and is of a network structure at its final polymerized form, which correlates to its shape memory property. A stick-shaped specimen was printed to evaluate the material's mechanical properties, with dimensions set to LW 60×14 mm. Considering the commonly used aligner thicknesses of 0.5 mm, 0.65 mm, and 0.8 mm, the specimens were printed with three thicknesses by using computer-aided design. Specimens were printed by the DLP 3D printer, Uniz 4 K (Uniz, San Diego, USA) with layer thickness of 100 μm and exposure time of 1.3 s for each layer. After printing, residual liquid resin on the specimen's surface was gently removed with a soft scraper, and the specimen was then cured using a post curing machine (Tera Harz Cure, Graphy Inc., Korea) for 20 min, using UV light within the wavelength range of 385–405 nm under Nitrogen condition<sup>36,52</sup>.

For Dynamic Mechanical Analysis (DMA) and Viscoelastic Testing, the specimen dimensions were customized to fit the capacity of the DMA equipment (Q800, TA Instrument, USA), which has a maximum load capability of 18 N. Rectangular strips with dimensions of and 5×40 mm for the TC-85 specimens. To ensure uniformity, the average thickness of the specimens was calculated by measuring the thicknesses at three points (two ends and the middle) along with the length of each specimen for each test and measurements.

### Static mechanical property test (Tensile test)

Tensile test was carried out on seven specimens from each group, immersed in a water bath of constant temperatures of 30 °C, 35 °C, 40 °C, and 45 °C, as illustrated in Fig. 1. The tensile test was conducted using a

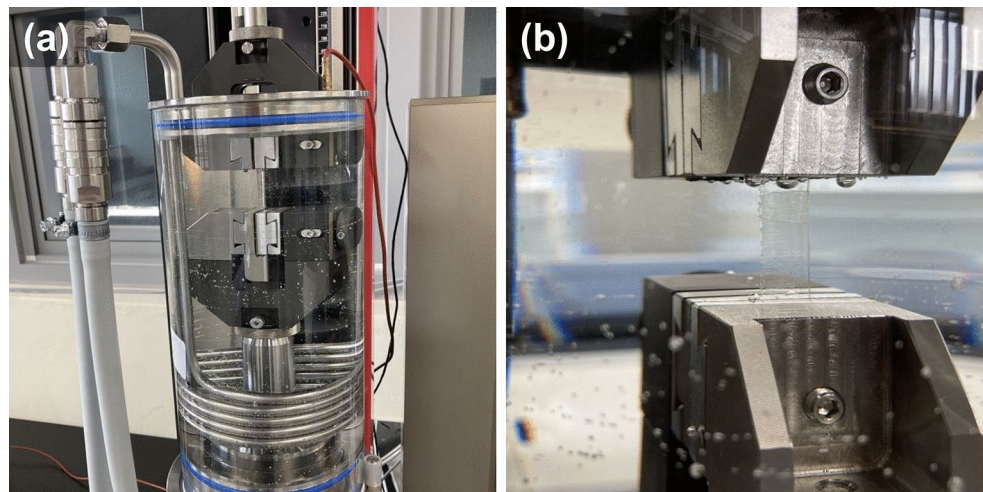


**Fig. 1.** Thermostatic water bath for universal testing machine for measuring tensile strength according to temperature change; **(a)** Configuration of constant temperature water bath, **(b)** Tensile test fixture.

Universal Testing Machine (AllroundLine Z010, 2 kN load cell, Zwick, Germany). Tension was applied to each specimen continuously until fracture with a crosshead speed of 5 mm/min. The static mechanical properties were evaluated by measuring the yield strength and elastic modulus.

### Dynamic mechanical property

#### *Dynamic mechanical analysis (DMA) test (Frequency sweep)*

To evaluate the rheological properties of the material, dynamic mechanical analysis (DMA) was conducted using a frequency sweep approach. Tests were performed at temperatures of 30 °C, 35 °C, 40 °C, and 45 °C, at a strain rate of 0.1%, and frequency range from 0.1 to 100 Hz. The heating rate was maintained at 5 °C/min (K/min), utilizing a DMA equipment (Q800, TA instrument, USA). Storage modulus, loss modulus, and loss tangent were measured in relation to temperature. The tests were then repeated three times for each temperature group to ensure reliability of the experiments with an error margin below 10%.

#### *thermo-mechanical cycle test (Stress relaxation & creep test)*

The evaluation of creep behavior and stress relaxation for each material was performed using DMA (Q800, TA instrument, USA) and its stress relaxation mode. The specimen was firmly positioned at supporting points to maintain a consistent distance of 10 mm between the fixation zig. Thirteen cycles were carried out, each involving 2% tension maintained for 60 min at temperatures of 30 °C, 35 °C, 40 °C, and 45 °C, each followed by a 60-min recovery period. This experimental design was also mainly referenced to prior research, which showed that 60 min of tension induced the most significant changes in the material's behavior<sup>39</sup>. Additionally, after the 10th cycle, the material's response reaches a point of saturation, and subsequent cycles show minimal changes<sup>39</sup>. Patterns of stress relaxation and strain recovery were methodically observed throughout the experiments. Importantly, three specimens at each temperature were subjected to repeated testing, confirming that the results from each experiment fell within a 10% error margin.

#### *Shape memory property test*

Among several methods of evaluating the shape recovery effect of materials, the bending test was chosen to qualitatively investigate and directly visualize the shape recovery property<sup>53,54</sup>. A U-shaped model was used to simulate a scenario in which a tooth deviates from the occlusal line towards the buccal side under the influence of a bending force exerted by aligners. The shape recovery rate is affected by the thickness of the specimen. Therefore, in order to observe meaningful shape recovery rate in the context of clinical applications, the test specimens had thicknesses within clinically relevant range of 0.5 mm to 0.7 mm. The central shaft of the U-shaped model had a diameter of 4 mm. Specimens were bent into a U-shape at 80 °C, which is above the glass transition temperature ( $T_g$ ) of TC-85 and were held in this position for 5 min (note:  $T_g$  values were ascertained via DMA)<sup>39</sup>. These specimens, once bent at this elevated temperature, were then quickly cooled to and maintained at 24 °C for additional 5 min. Upon removing the external force, the initial bending angle ( $\theta_{initial}$ ) of the folded specimen was measured. Then, the specimens were immersed in a water bath at temperatures of 30 °C, 35 °C, 40 °C, and 45 °C, where the shape recovery process was recorded using video capture at a frame rate of 30 FPS over an hour. The initial bending angle ( $\theta_{initial}$ ) and the bending angle at subsequent times ( $\theta_t$ ) were measured at specified time intervals (10 s, 30 s, 1 min, 5 min, 10 min, 30 min, and 60 min) using the mathematics software GeoGebra, developed by Markus Hohenwarter. The shape recovery ratio was determined using the following equation:

$$\text{Shaperecoveryratio} = \frac{\theta_{initial} - \theta_t}{\theta_{initial}} * 100\%$$

## Result

As temperature rose from 30°C to 45°C, a gradual decrease in tensile strength, elastic modulus, and maximum force within a 20% strain was noted. The tensile strength and elastic modulus did not show significant change with varied sample thicknesses (Figs. 2a and 2b). However, for max standard force, the thicker specimen showed much higher max standard force in 20% at 30 °C. However, with increasing temperature, this difference diminished, and beyond 40°C, the relationship between max standard force and thickness was not significant (Fig. 2c). Figure 2d displays the elongation at break in relation to both temperature and sample thickness, with all elongation values exceeding 100% and showing large standard deviations.

The force distribution resulting from an applied tensile load in relation to thickness and temperature is demonstrated in Fig. 3. The results indicate that the force required for deformation significantly decreases as temperature increases from 30°C to 45°C for all thicknesses. The force deviation based on temperature was the most pronounced in the specimen with 0.8 mm thickness, aligning with the observations in Fig. 2c.

Figure 4 presents changes in storage modulus and loss modulus from the DMA frequency sweep at varying temperatures. A distinct decrease in storage modulus was noted as the temperature increases from 30°C to 40°C, but at temperatures beyond 40°C, no significant decrease in storage modulus nor increase in loss modulus was observed.

The cycle tests, involving a 2% elongation held for 60 min, followed by a 60-min force release period, showed the pattern of stress relaxation based on temperature (Fig. 5). Specimens exposed to temperatures over 40°C seemed to recover fully to their original form, coupled with a reduction in the magnitude of the applied force. The inherent stress and recovery rates after 13 cycles are detailed in Table 1. At the end of the 1 h recording, specimens at 30°C and 35°C exhibited a recovery rate below 80%, whereas those above 40°C, especially at 45°C, showed a recovery rate above 90%, suggesting nearly complete recovery and significant stress relaxation.

The results of the shape memory experiments highlighted the temperature-dependent behaviors of the material. According to the 1 h observation of shape recovery, the materials showed the fastest recovery was at 45 °C reaching 99% recovery, while the slowest was at 30 °C, where only 34.4% recovery occurred after 60 min

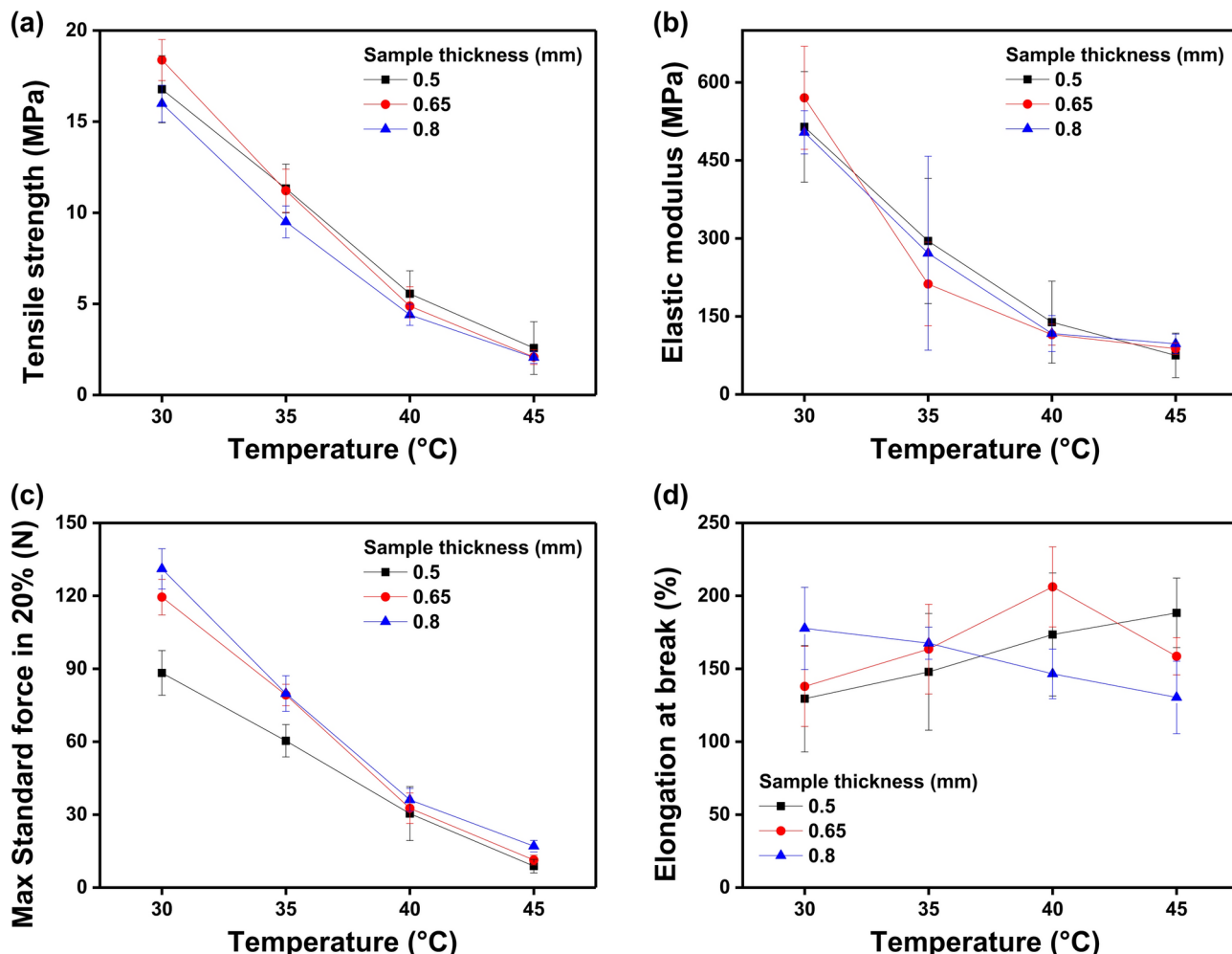


**Fig. 2.** Test result of tensile strength according to thickness and temperature change of tensile specimen in constant temperature water bath of universal testing machine; (a) tensile strength, (b) tensile modulus, (c) maximum tensile force within 20% strain, (d) maximum elongation break.

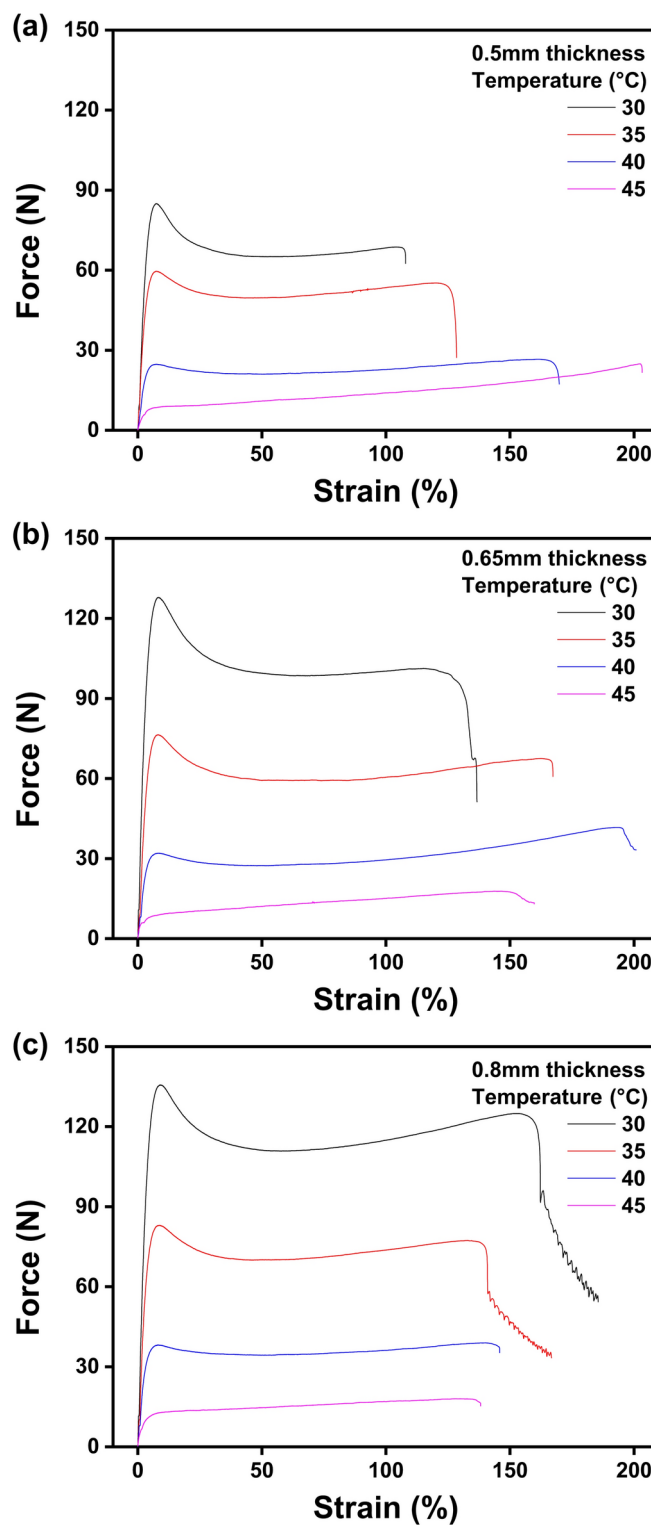


**Fig. 3.** Stress–strain graph of tensile strength according to thickness and temperature change of tensile specimen in a constant temperature water bath of universal testing machine; (a) 0.5 mm, (b) 0.65 mm, (c) 0.8 mm.

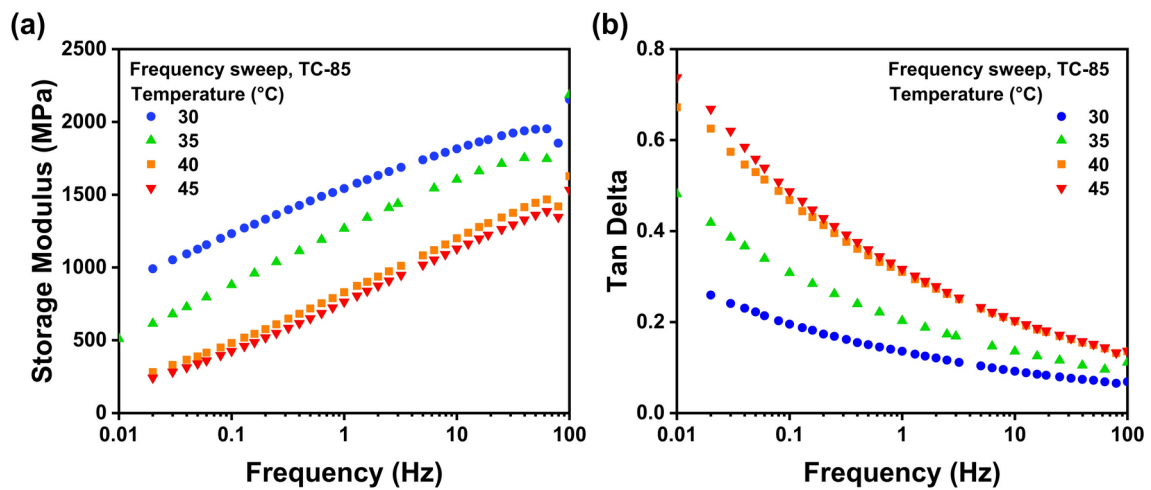


**Fig. 4.** Rheological property change test according to frequency sweep for each temperature using DMA; (a) storage modulus, (b) loss modulus.

(Fig. 6). The calculated values of shape recovery ratio of TC-85 specimens based on the measured initial bending angles ( $\theta_{\text{initial}}$ ) and bending angles at subsequent times ( $\theta_t$ ) are shown in Table 2 and Fig. 7.

## Discussion

In contrast to previous study that used dumbbell-shaped specimens for tensile test, this research employed stick-shaped specimens to minimize experimental bias due to variations in specimen dimensions and sample loss<sup>39</sup>. In orthodontics, clear aligners are typically thin (less than 1 mm in thickness), and their mechanical behavior in a clinical setting is influenced by factors such as tensile strength, elongation, and flexibility. To better simulate the conditions of real aligners, we selected specimens with a thickness similar to that of actual aligners. This decision was made to ensure that our experimental conditions closely mimic the real-world mechanical behavior of orthodontic aligners, which are commonly used in clinical practice. According to ISO 527-3 and ASTM D882 standards for tensile test for films of whose specimen thickness is below 1 mm, it is recommended to use a rectangular shape instead of the traditional dumbbell form. This adjustment allowed us to better reflect the clinical situation and the material behavior in real orthodontic aligners. Additionally, from our pilot studies, dumbbell-shaped specimens became more prone to damage during sample preparation when the thickness was reduced. This could also affect the reproducibility and repeatability of the experiment, as well as the overall reliability of the data. The rectangular shape helped mitigate these issues and ensured more consistent specimen handling and preparation.

The initial hypothesis applied to the previous study was that variations in the thickness of clear aligner devices could lead to unwanted forces on the teeth, with the assumption that aligner thickness significantly affects the orthodontic forces applied. However, results from the previous study focused on the differences in physical properties between PETG and TC-85 rather than addressing the differences in physical properties based on thickness variations<sup>39</sup>. In this study, only one material was used, and the hypothesis was empirically tested by fabricating TC-85 specimens at three thicknesses of 0.5 mm, 0.65 mm, and 0.8 mm.

One of the most significant findings from previous research is that the physical properties of materials, especially TC-85, demonstrate very particular viscoelastic behaviors and temperature-dependent shape memory properties<sup>25,26,39</sup>. Experiments were conducted at 37 °C and 80 °C to test the properties near body temperature. However, temperature such as 80 °C above  $T_g$  was a condition too extreme to compare the changed properties to draw clinical meaning. The current study sought to rectify this by evaluating material properties at temperatures that are more representative of conditions within the oral cavity on a daily basis: 30 °C, 35 °C, 40 °C, and 45 °C.

Theoretically, tensile strength and elastic modulus are derived from maximum tensile and cross-sectional area of the material, thus are independent of the thickness. The current study corroborated this, showing no significant variance in these measurements across different thicknesses. However, a clear trend was observed whereby an increase in temperature led to a decrease in both tensile strength and elastic modulus, which in turn made the material more ductile, requiring less force for deformation. Unlike vacuum formed clear aligners made of materials such as PETG, direct printed aligners can be designed to fit dental anatomy precisely regardless of undercuts<sup>7,14,23</sup>. This allows close fit along all surface between the device and teeth, providing more effective orthodontic force<sup>7,12,25,26,45,50,55–57</sup>. However, the perfect fit requires the device to pass through the height of contour and reach the undercut area. For optimal placement, the device must be able to adapt to dental contours and undercuts with minimal force and have adequate flexibility to avoid discomfort or breakage during the application or removal process. Therefore, lower tensile strength and elastic modulus are considered preferable. Additionally, the temperature-dependent flexibility can be used in advantage to ease the fitting and removal process of the device. For example, the device can be heated in hot water before fitting and heated by drinking warm water above body temperature before removing in order to increase flexibility instantly and ease the tight fit to fit and remove with minimal force required.

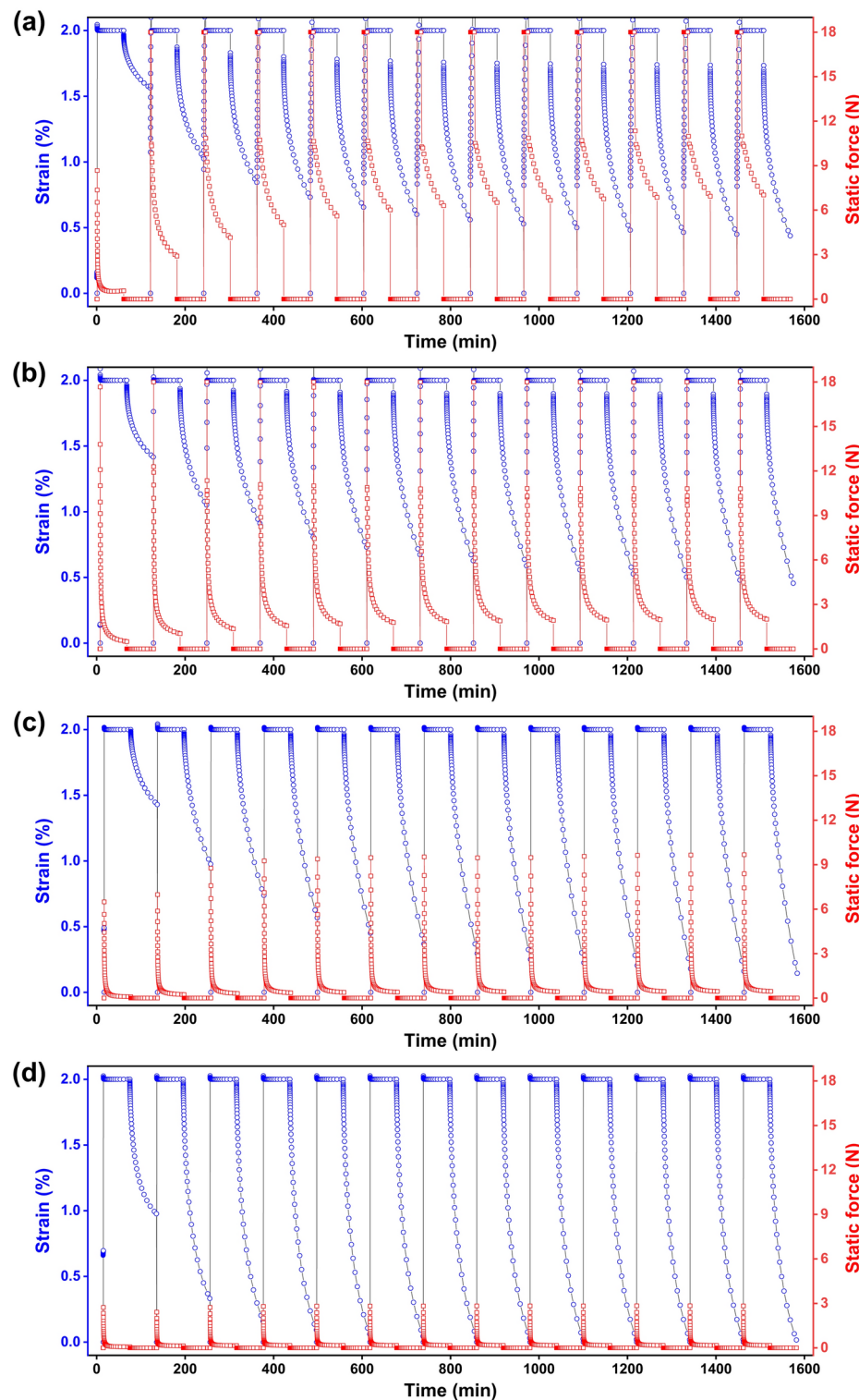


**Fig. 5.** Stress relaxation and creep at 30, 35, 40 °C and 45 °C; The cycle of 2% elongation for 60 min and recovery for 60 min was repeated 13 cycles; (a) 30 °C; (b) 35 °C; (c) 40 °C; (d) 45 °C.

Maximum standard force is measured in order to investigate the physical properties with thickness factor as an added factor. It was discovered that actual tensile strength varies with the thickness of the device, implying that thinner devices require smaller force for deformation. In clinical settings where the aligner is to be applied to areas with poor periodontal health or sever undercuts, thinner device would be more advantageous for avoiding applying large force. Although a trend of decreasing force required with increasing temperatures was noted across all thicknesses, no substantial differences were observed above 40 °C. Also, the force difference

Temperature (°C)	Static force (N)	Recovery rate (%)
30	7.02	78.11
35	2.00	77.20
40	0.45	92.76
45	0.18	99.18

**Table 1.** Static force and recovery rate at 30 °C, 35 °C, 40 °C and 45 °C at the 13th stress relaxation and creep of 13 repetitions of a cycle of 2% elongation for 60 min and recovery for 60 min.

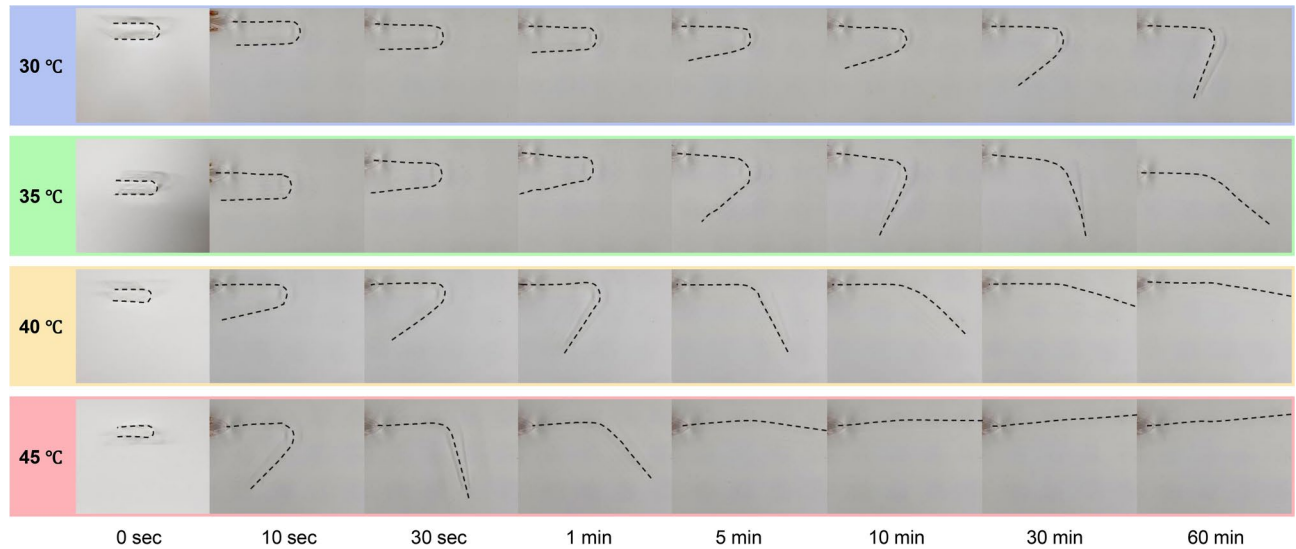


**Fig. 6.** Shape memory effect over time of TC-85.

Temperature	Elapsed time							
	0 s	10 s	30 s	60 s	300 s	600 s	1800s	3600 s
30 °C	0	0.7±0.4	1.3±0.5	2.1±0.7	7.6±1.8	11.5±1.3	23.1±2.7	34.4±2.6
35 °C	0	1.6±1	5.2±0.9	8.2±1.6	25.8±3.5	38.3±3.6	62.6±2.8	78.1±2.9
40 °C	0	6.8±0.8	17.4±2.4	27.3±3.8	60.1±5.3	74±3.4	90.1±0.6	95.5±1.4
45 °C	0	26.9±4	54.7±4.8	70.9±7.1	90.9±3.2	95.7±1.1	98.5±1	99.2±0.9

**Table 2.** Shape recovery ratio (%) of TC-85 specimens at 0 s, 10 s, 30 s, 1 min, 5 min, 10 min, 30 min and 1 h at different temperatures (N = 3).

between 0.65 mm specimen and 0.8 mm specimen was relatively small at 30 °C and 35°C. Therefore, while the thickness of the device does have some effect on the orthodontic corrective force exerted on teeth, its clinical significance seems insignificant.

A stress-strain curve was created to visually demonstrate force variations relative to temperature (Fig. 3). As previously explained, force required for same strain decreased with increased temperature for a given thickness. Although the graph shows how the material behaves until its elongation break, only the initial values of the curve is clinically meaningful, because actual tooth movement occurs within a narrow range of elongation, making values beyond the initial changes less critical in clinical relevance. Similar to the results from previous study, all specimen reached its peak force in the beginning stage of deformation<sup>39</sup>. Compared to peaks of PETG, TC-85 showed significantly lower peak force. This result corroborates the potential of TC-85 to facilitate efficient tooth adjustment with fewer steps and biologically more suitable force. Applying this finding to clinical settings, the thicker the device is, the more movement per step one give. However, thickness over 0.65 mm is expected to have no significant effect. Also, since the material's flexibility is temperature-dependant, it is possible to minimize side effects and discomfort especially when using an aligner designed for large tooth movement by utilizing warm temperature over body temperature and introducing physiological force to the teeth.

As shown in Fig. 4, the temperature increases by 5 °C from 30 °C to 45 °C, storage modulus decreases and tan delta increases. This phenomenon is very natural because it is based on the softening of polymers due to temperature change and also aligns with previous works<sup>25,39</sup>. However, in case of an orthodontic device,

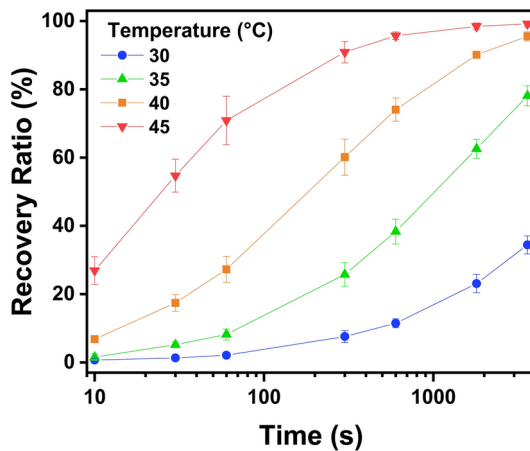


**Fig. 7.** Recovery ratio (%) of TC-85 with respect to time (s) in log scale at varied temperatures of 30 °C, 35 °C, 40 °C, and 45 °C.

the temperature at which the viscoelastic properties are maximized must be around 35 °C near human body temperature. In this study, as the temperature rises from 30 °C to 40 °C, the decrease of storage modulus and increase of tan delta occur at a constant rate, but the rate is hindered when the temperature rises above 40 °C. Such phenomenon generally occurs around the Tg (glass transition temperature) of polymer materials. It can be inferred that the viscoelastic properties of the material are maximized in an environment at 35 °C in the oral cavity near its Tg.

Stress relaxation and creep of TC-85 were examined at 2% strain rate to mimic the material deformation during the application of the device (Fig. 5). In the previous study, experiments were conducted under a 1% strain rate condition, which was an inevitable condition due to the low elasticity of PETG<sup>39</sup>. However, focus of this study was to investigate the effect of temperature by using only the TC-85 material, which has high flexibility and correspondingly high elastic range, so the experiments could be conducted at a strain rate of 2%. As the cycles progressed, stress relaxation became evident when the temperature was higher, and the static force also tended to decrease immediately. According to the results of the previous experiment, the amplitude of the initial force tended to be larger at lower temperature, and the static force in stress relaxation condition was also relatively higher at lower temperature<sup>39</sup>. In addition, the creep occurred more clearly at lower temperatures and static force continuously increased as the cycle progressed. From a biomechanical perspective, creep could be seen as beneficial since it minimizes force decay and sustains the orthodontic force applied by the aligners.

These results show that in a clinical situation where the orthodontic device is worn and placed under continuous strain, the force exerted from the device to the teeth can be changed with temperature. When a patient wears the aligner, appropriate orthodontic force must be applied to the teeth, and it must occur at a temperature close to oral environment approximately at 35 °C. Combined with the results from the previous studies which involves long-term exposure to oral conditions and liquids<sup>12,37,38,45,47,55,58</sup>, the higher strain rate resulted in greater force. Therefore, by individualizing movement of each tooth in the set-up process and adjusting the expected strain rate, the ideal orthodontic force can be achieved with specifically controlled applied forces<sup>55,56</sup>. If the patient experiences pain when installing the device, using water at a temperature higher than body temperature can help by immediately lowering the applied force to 0 N.

There may be concerns about permanent deformation of the device due to creep phenomenon and repeated use<sup>14,23,37</sup>. However, these concerns could be dismissed by the previous research which confirmed the shape memory property of the newly developed material at 37°C and 80°C followed by this study attempted to look at the shape memory pattern under more detailed conditions<sup>39</sup>. Likewise, the material exhibited quicker recovery at an elevated temperature (Table 2). This study provides detailed pattern of shape memory and suggests that warming the clear aligner may be used as a guideline for first-timers and patients in transitions between orthodontic stages to lessen the discomfort.

With TC-85, it is possible to control the applied force more precisely by thickness variations within an aligner or by incorporating negative attachments rather than adhesive attachment to the teeth or using multi-layer sheets. In the case of thermoformed aligners made with PETG materials, 1 kg tension was generated at a strain rate of 1%, but direct printed aligner generated a force of 100 g at 1% and 200 g at 2%. Such orthodontic-friendly force range allows the operator to freely plan the orthodontic treatment without concerns on excessive amount of force. This method can be expressed as a force driven system. Even if the oral temperature rises by just 5 degrees, the orthodontic corrective force is clearly released and returns in moderate measures that is more biomechanically suitable.

In conclusion, the immediate force when applying the device at body temperature may surpass physiological force. This is a common phenomenon among existing clear aligners, and materials such as PETG exert much greater initial force<sup>12</sup>. However, more efficient tooth movement is ensured with the property of TC-85 which allows stress relaxation to occur immediately and exert the most physiological force. Therefore, when using the device for the first time, it is advised to use it at a higher initial temperature to minimize discomfort and

prevent excessive forces. Then, gradual adjustment to oral cavity temperature will ensure a smooth transition to physiological force range for optimal orthodontic corrective force applications.

Although the study examined material properties across various temperatures, different clinical conditions, varying orthodontic clear aligner materials, simulation of installation and removal of the device, long-term exposure to oral conditions, and the orthodontic force under fluctuating temperature rather than a fixed temperature in order to derive more clinically meaningful results. Also, since the water was involved in the tensile test, water sorption properties could be included in future studies as response to water exposure is a significant factor for orthodontic devices. In addition, further investigation is necessary on various teeth morphologies and health conditions of periodontal tissues to determine how much tooth movement per set is appropriate to achieve the 1% and 2% strain as assumed in this and previous studies.

Looking ahead, several promising approaches could expand the use of TC-85 in orthodontics and beyond. Surface treatments with carboxybetaine-copolymers have demonstrated significant improvements in biofilm resistance while maintaining the optical translucency of 3D printed clear aligners, which is crucial for long-term device cleanliness and patient comfort<sup>59</sup>. Furthermore, the integration of acrylated cellulose nanocrystals (A-CNCs) into TC-85-based photocurable resins has shown enhancements in mechanical properties, transparency, and shape-memory performance<sup>60</sup>. This opens up new possibilities for developing strong, transparent, and bioresponsive materials. Additionally, a recent work introduced an innovative workflow that pairs AI-driven CBCT segmentation with temperature-responsive 4D polymers (TC-85) to create patient-specific bioengineered scaffolds<sup>61</sup>. These AI-aided designs, when combined with TC-85, have shown promising results for personalized applications beyond orthodontics in fields like orthopedics, dental implants, and tissue engineering. AI could play a crucial role in personalizing the design and performance of biomedical materials, enabling precise customization to patient-specific needs. These combined advancements in surface treatments, material composites, and AI-driven design pave the way for the future of TC-85 in personalized, high-performance medical devices.

## Conclusions

1. TC-85, sensitive to body temperature, showcases enhanced shape memory with rising temperatures, reducing the corrective force of clear aligners for improved patient comfort.
2. At 45 °C, TC-85 reaches peak flexibility, aiding in comfortable orthodontic correction, while below 30 °C, it maintains stiffness and resistance to external deformation.
3. At 30 °C, TC-85's elasticity, stress relaxation, and strain recovery properties enable it to deliver a steady, gentle corrective force suitable for orthodontic treatment.
4. TC-85 resists force decay under varied thermal conditions, maintaining its corrective effectiveness through multiple device applications and removals.
5. With TC-85, it is possible to control the applied force more precisely by thickness variations rather than adhesive attachments or multi-layer sheets due to direct 3D printing.
6. The stable, cross-linked structure of TC-85 remains consistent at 80 °C, providing advantages over PETG in durability and user maintenance.

## Limitation

1. The outcomes may differ under conditions of 100% humidity, similar to those in the oral cavity, due to the considerable water absorption characteristic of polyurethane.
2. Prolonging the stress relaxation test beyond 24 h could provide more significant findings that better reflect the typical wear duration of orthodontic aligners, which usually exceeds 24 h.

## Data availability

The datasets used and/or analysed during the current study available from the corresponding author on reasonable request.

Received: 15 March 2024; Accepted: 4 March 2025

Published online: 02 July 2025

## References

1. Clear Aligners Market Size, Share, Growth | Forecast, 2024–2032 <https://www.fortunebusinessinsights.com/industry-reports/clear-aligners-market-101377>
2. Ojima, K. & Kau, C. H. A perspective in accelerated orthodontics with aligner treatment. *Semin. Orthod.* **23**, 76–82 (2017).
3. Mulli Issa, F. K., Mulli Issa, Z. K., Rabah, A. & Hu, L. Periodontal parameters in adult patients with clear aligners orthodontics treatment versus three other types of brackets: A cross-sectional study. *J. Orthod. Sci.* **9**, 4 (2020).
4. Robertson, L. et al. Effectiveness of clear aligner therapy for orthodontic treatment: A systematic review. *Orthod. Craniofac. Res.* **23**, 133–142 (2020).
5. Rossini, G., Parrini, S., Castroflorio, T., Deregbus, A. & Debernardi, C. L. Efficacy of clear aligners in controlling orthodontic tooth movement: A systematic review. *Angle Orthod.* **85**, 881–889 (2015).
6. Djeu, G., Shelton, C. & Maganzini, A. Outcome assessment of Invisalign and traditional orthodontic treatment compared with the American board of orthodontics objective grading system. *Am. J. Orthod. & Dentofac. Orthop.* **128**, 292–298 (2005).
7. Alkhamees, A. The new additive era of orthodontics: 3D-printed aligners and shape memory polymers—the latest trend—and their environmental implications. *J. Orthod. Sci.* [https://doi.org/10.4103/jos.jos\\_211\\_23](https://doi.org/10.4103/jos.jos_211_23) (2024).
8. Cremonini, F. et al. A Spectrophotometry evaluation of clear aligners transparency: Comparison of 3D-Printers and thermoforming disks in different combinations. *Appl. Sci.* **12**, 11964 (2022).
9. Thukral, R. & Gupta, A. Invisalign: Invisible orthodontic treatment—a review. *J. Adv. Med. & Dent. Sci. Res.* **3**(5), S42s (2015).

10. Ercoli, F., Tepedino, M., Parziale, V. & Luzi, C. A comparative study of two different clear aligner systems. *Prog. Orthod.* <https://doi.org/10.1186/s40510-014-0031-3> (2014).
11. Momtaz, P. The effect of attachment placement and location on rotational control of conical teeth using clear aligner therapy. (2016).
12. Author, C. et al. Force assessment of thermoformed and direct-printed aligners in a lingual bodily movement of a central incisor over time: A 14-day in vitro study. *J. Korean Dent. Sci.* **16**, 23–34 (2023).
13. Ghoraba, O. et al. Effect of the height of a 3D-printed model on the force transmission and thickness of thermoformed orthodontic aligners. *Materials* **17**, 3019 (2024).
14. Koenig, N. et al. Comparison of dimensional accuracy between direct-printed and thermoformed aligners. *Korean J Orthod.* **52**, 249–257 (2022).
15. Seeger, P., Ratschisch, R., Moneke, M. & Burkhardt, T. Addition of thermo-plastic polyurethane (TPU) to poly (methyl methacrylate) (PMMA) to improve its impact strength and to change its scratch behavior. *Wear* **406**, 68–74ss (2018).
16. Zhang, N., Bai, Y., Ding, X. & Zhang, Y. Preparation and characterization of thermoplastic materials for invisible orthodontics. *Dental Mater. J.* **30**(6), 954–959ss (2011).
17. Yan Song, M. A. et al. Mechanical properties of orthodontic thermoplastics PETG/PC2858 after blending Chin. *J. Dent. Res.* **19**(43), 48s (2016).
18. B Suresha, JH Lee Mechanical and three-body abrasive wear behaviour of PMMA/TPU blends *Materials Science and Engineering: A* **2008 Elsevier**
19. Hwang, S. H., Jeong, K. S. & Jung, J. C. Thermal and mechanical properties of amorphous copolyester (PETG)/LCP blends. *Eur. Polym. J.* **35**(8), 1439–1443 (1999).
20. Medellin-Rodríguez, F. J., Phillips, P. J., Lin, J. S. & Avila-Orta, C. A. Triple melting behavior of poly (ethylene terephthalate co-1,4-cyclohexylene dimethylene terephthalate) random copolymers. *J. Polym. Sci. Part B: Polym. Phys.* **36**(5), 763–781 (1998).
21. Cole, D., Bencharit, S., Carrico, C. K., Arias, A. & Tüfekçi, E. Evaluation of fit for 3D-printed retainers compared with thermoform retainers. *Am. J. Orthodont. & Dentofac. Orthop.* **155**(4), 592–599 (2019).
22. Jindal, P., Juneja, M., Siena, F. L., Bajaj, D. & Breedon, P. Mechanical and geometric properties of thermoformed and 3D printed clear dental aligners. *Am. J. Orthod. & Dentofac. Orthop.* **156**, 694–701 (2019).
23. Park, S. Y. et al. Comparison of translucency, thickness, and gap width of thermoformed and 3D-printed clear aligners using micro-CT and spectrophotometer. *Sci. Rep.* <https://doi.org/10.1038/s41598-023-36851-5> (2023).
24. Narongdej, P., Hassanpour, M., Alterman, N., Rawlins-Buchanan, F. & Barjasteh, E. Advancements in clear aligner fabrication: A comprehensive review of direct-3D printing technologies. *Polymers* **16** Preprint at <https://doi.org/10.3390/polym16030371> (2024)
25. Atta, I. et al. Physicochemical and mechanical characterisation of orthodontic 3D printed aligner material made of shape memory polymers (4D aligner material). *J. Mech. Behav. Biomed. Mater.* **150**, 106337 (2024).
26. Schupp, W. et al. Shape memory aligners: A new dimension in aligner orthodontics. *J. Aligner Orthod.* **7**(2), 113–127 (2023).
27. Bichu, Y. M. et al. Advances in orthodontic clear aligner materials. *Bioact. Mater.* **22**, 384–403 (2023).
28. Slaymaker, J., Hirani, S. & Woolley, J. Direct 3D printing aligners-past, present and future possibilities. *Br. Dent. J.* **236**(5), 401–405 (2024).
29. Panayi, N. C., Efstathiou, S., Christopoulou, I., Kotantoula, G. & Tsolakis, I. A. Digital orthodontics: Present and future. *AJO-DO Clin. Companion* **4**(1), 14–25 (2024).
30. Andreu, A. et al. 4D printing materials for vat photopolymerization. *Addit. Manuf.* **44**, 102024 (2021).
31. Campobasso, A. et al. Comparison of the cytotoxicity of 3D-printed aligners using different post-curing procedures: An in vitro study. *Aust. Orthod. J.* **39**, 49–56 (2023).
32. Kim, H., Khan, T. A., Ryu, K.-H., Sohn, I.-S. & Kim, H.-J. Nanocomposite materials for 3D printing. In Ahmed, W. & Maciel, M. A. M.(eds) *Applications And Industrialisation Of Nanotechnology* 91–118 (2022)
33. Lee, J. et al. Average-accumulated normalized dose (A-AND) predicts ultimate tensile strength and elastic modulus of photopolymer printed by vat photopolymerization. *Addit. Manuf.* **55**, 102799 (2022).
34. Kim, H. et al. 3D printing of polyethylene terephthalate glycol–sepiolite composites with nanoscale orientation. *ACS Appl. Mater. Interfaces* **12**, 23453–23463 (2020).
35. Kim, H. et al. Embedded direct ink writing 3D printing of uv curable resin/sepiolite composites with nano orientation. *ACS Omega* **8**, 23554–23565 (2023).
36. Šimunović, L. et al. Influence of post-processing on the degree of conversion and mechanical properties of 3D-printed polyurethane aligners. *Polymers (Basel)* <https://doi.org/10.3390/polym16010017> (2024).
37. Papadopoulou, A. K., Cantele, A., Polychronis, G., Zinelis, S. & Eliades, T. Changes in roughness and mechanical properties of invisalign® appliances after one- and two-weeks use. *Materials* <https://doi.org/10.3390/ma12152406> (2019).
38. Sari, T., Camci, H. & Aslantaş, K. Evaluation of mechanical changes to clear aligners caused by exposure to different liquids. *Aust. Orthod. J.* **40**, 75–86 (2024).
39. Lee, S. Y. et al. Thermo-mechanical properties of 3D printed photocurable shape memory resin for clear aligners. *Sci. Rep.* <https://doi.org/10.1038/s41598-022-09831-4> (2022).
40. Sivak, M. G., Jo, Y.-M., Nanda, R. & Bechtold, T. E. *In-House 3D-Printed Shape Memory Aligners for Retreatment after Fixed Retainer Failure*. [www.jco-online.com](http://www.jco-online.com) (2024).
41. Viet, H., Lam, T. H., Phuc, N. N., Ngoc Lenh, N. & Thao, D. T. N. Class II correction and crowding treatment using in-house direct printed clear aligners: A literature review and case report. *Cureus* <https://doi.org/10.7759/cureus.65024> (2024).
42. Hoang, V., Dang, T. T. N., Nguyen, M. K. & Tran, P. H. (2024) Accelerated and hybrid orthodontic treatment using a combination of 2D lingual appliance and in-house aligner: An anterior cross-bite and TMD case report after 1-year follow-up *APOS Trends in Orthodontics* **0** 1–7
43. Knodel, V. et al. Directly printed aligner therapy: A 12-month evaluation of application and effectiveness. *Am. J. Orthod. & Dentofac. Orthop.* **167**, 73–79 (2025).
44. Ludwig, B., Ojima, K., Schmid, J. Q., Knodel, V. & Nanda, R. *Direct-Printed Aligners: A Clinical Status Report Clinical Uses* [www.jco-online.com](http://www.jco-online.com) (2024)
45. Hertan, E., McCray, J., Bankhead, B. & Kim, K. B. Force profile assessment of direct-printed aligners versus thermoformed aligners and the effects of non-engaged surface patterns. *Prog. Orthod.* <https://doi.org/10.1186/s40510-022-00443-2> (2022).
46. Elshazly, T. M. et al. Effect of thermomechanical aging of orthodontic aligners on force and torque generation: An in vitro study. *J. Mech. Behav. Biomed. Mater.* **143**, 105911 (2023).
47. Fang, D., Zhang, N., Chen, H. & Bai, Y. Dynamic stress relaxation of orthodontic thermoplastic materials in a simulated oral environment. *Dent. Mater. J.* **32**, 946–951 (2013).
48. Kravitz, N. D., Kusnoto, B., BeGole, E., Obrez, A. & Agran, B. How well does Invisalign work? A prospective clinical study evaluating the efficacy of tooth movement with Invisalign. *Am. J. Orthod. & Dentofac. Orthop.* **135**, 27–35 (2009).
49. Lombardo, L. et al. Stress relaxation properties of four orthodontic aligner materials: A 24-hour in vitro study. *Angle Orthod.* **87**, 11–18 (2016).
50. Sharif, M. et al. Force system of 3D-printed orthodontic aligners made of shape memory polymers: An in vitro study. *Virtual Phys. Prototyp.* **10**(1080/17452759), 2361857 (2024).
51. Longman, C. M. & Pearson, G. J. Variations in tooth, surface temperature in the oral cavity during fluid intake. *Biomaterials* **8**, 411–414 (1987).

52. Lim, B. et al. Influence of post-curing in nitrogen-saturated condition on the degree of conversion and color stability of 3D-printed resin crowns. *Dent. J. (Basel)* **12**(3), 68 (2024).
53. Wang, Z., Liu, J., Guo, J., Sun, X. & Xu, L. The study of thermal mechanical and shape memory properties of chopped carbon fiber-reinforced TPI shape memory polymer composites. *Polym. (Basel)* **9**(11), 594 (2017).
54. Liu, Y. et al. Thermo-mechanical properties of glass fiber reinforced shape memory polyurethane for orthodontic application. *J. Mater. Sci. Mater. Med.* **29**, 148 (2018).
55. McKay, A. et al. Forces and moments generated during extrusion of a maxillary central incisor with clear aligners: An in vitro study. *BMC Oral Health* <https://doi.org/10.1186/s12903-023-03136-2> (2023).
56. Grant, J. et al. Forces and moments generated by 3D direct printed clear aligners of varying labial and lingual thicknesses during lingual movement of maxillary central incisor: an in vitro study. *Prog. Orthod.* <https://doi.org/10.1186/s40510-023-00475-2> (2023).
57. Elshazly, T. M. et al. Primary evaluation of shape recovery of orthodontic aligners fabricated from shape memory polymer (A typodont study). *Dent. J. (Basel)* <https://doi.org/10.3390/dj9030031> (2021).
58. Can, E. et al. In-house 3D-printed aligners: Effect of in vivo ageing on mechanical properties. *Eur. J. Orthod.* **44**, 51–55 (2022).
59. Wu, C. et al. Enhancing biofilm resistance and preserving optical translucency of 3D printed clear aligners through carboxybetaine-copolymer surface treatment. *Dent. Mater.* **40**, 1575–1583 (2024).
60. Choi, J. et al. Incorporation of acrylated cellulose nanocrystals into photocurable resin for high-fidelity printing of transparent 3D structures. *J. Manuf. Process* **139**, 1–11 (2025).
61. Thurzo, A. & Varga, I. Advances in 4D shape-memory resins for AI-aided personalized scaffold bioengineering. *Bratisl. Med. J.* <https://doi.org/10.1007/S44411-025-00043-6/FIGURES/1> (2025).

## Acknowledgements

Experiments were carried out through free support of Anton Paar Korea's rheometer test equipment, and we would like to thank to Anton Paar Korea for helping us.

## Author contributions

J.C., H.K., and K.K. conceptualized the study. H.K., J.M., and S.L. conducted the experiments. J.C. performed data analysis. H.K and S.L. prepared the figures. H.K. and J.L. wrote the manuscript with supervision of K.K. All authors reviewed the manuscript.

## Declarations

### Competing interests

The authors declare no competing interests.

### Additional information

**Correspondence** and requests for materials should be addressed to K.B.K.

**Reprints and permissions information** is available at [www.nature.com/reprints](http://www.nature.com/reprints).

**Publisher's note** Springer Nature remains neutral with regard to jurisdictional claims in published maps and institutional affiliations.

**Open Access** This article is licensed under a Creative Commons Attribution-NonCommercial-NoDerivatives 4.0 International License, which permits any non-commercial use, sharing, distribution and reproduction in any medium or format, as long as you give appropriate credit to the original author(s) and the source, provide a link to the Creative Commons licence, and indicate if you modified the licensed material. You do not have permission under this licence to share adapted material derived from this article or parts of it. The images or other third party material in this article are included in the article's Creative Commons licence, unless indicated otherwise in a credit line to the material. If material is not included in the article's Creative Commons licence and your intended use is not permitted by statutory regulation or exceeds the permitted use, you will need to obtain permission directly from the copyright holder. To view a copy of this licence, visit <http://creativecommons.org/licenses/by-nc-nd/4.0/>.

© The Author(s) 2025